Domain-wall excitations in the one-dimensional spin-$\frac{1}{2}$ fully anisotropic Ising-like antiferromagnet

1996 J. Phys.: Condens. Matter 8 351

(http://iopscience.iop.org/0953-8984/8/3/013)

J. Phys.: Condens. Matter **8** (1996) 351–360. Printed in the UK

Domain-wall excitations in the one-dimensional spin-$\frac{1}{2}$ fully anisotropic Ising-like antiferromagnet

Indrani Bose and Asimkumar Ghosh

Department of Physics, Bose Institute, 93/1 Acharya Prafulla Chandra Road, Calcutta-700 009, India

Received 3 May 1995, in final form 26 September 1995

Abstract. We consider the $S = \frac{1}{2}$ Ising-like, fully anisotropic Heisenberg antiferromagnetic Hamiltonian in one dimension and study the dynamics of domain-wall excitations using perturbation theory. It is shown that the domain walls can form bound states. The transverse correlation function $S^{xx}(\boldsymbol{q}, \omega)$ is calculated in first-order perturbation theory and the zone-centre lineshape is found to be asymmetric towards lower energy. A comparison of the results with earlier theories as well as experimental results on $CsCoCl_3$ and $CsCoBr_3$ is made.

1. Introduction

The $S = \frac{1}{2}$ Ising-like antiferromagnetic (AFM) chain has been extensively studied over the years [1–9]. The spin dynamics of the system are characterized by propagating domain walls or solitons. The exchange interaction Hamiltonian describing the system is given by

$$H = 2J \sum_i [S_i^z S_{i+1}^z + \varepsilon(S_i^x S_{i+1}^x + S_i^y S_{i+1}^y)] \qquad 0 < \varepsilon < 1. \tag{1}$$

Two experimental realizations of the model system are $CsCoCl_3$ and $CsCoBr_3$. For very small ε, the lowest-order ground state of (1) is the Néel state (figure 1) with a total z component of the spin given by $S_T^z = 0$. A domain-wall pair (DWP) state is created by flipping ν adjacent spins in the Néel state (figure 1). The first excited states with $S_T^z = 0, \pm 1$ consist of superpositions of the DWP states. Ishimura and Shiba (IS) [2] showed, using first-order perturbation theory in ε, that the propagating DWPs give rise to an excitation continuum around the Ising excitation energy $2J$. The existence of this continuum has been verified in inelastic neutron scattering experiments. At low temperatures, the spin-wave response measured near $\omega \sim 2J$ arises from transitions from the ground state to the first excited states. The response is determined by the transverse correlation function $S^{xx}(\boldsymbol{q}, \omega)$. At temperatures, when the DWP states are thermally populated, transitions within the band of excited states occur, giving rise to the so-called 'soliton response' in neutron scattering experiments. The longitudinal correlation function $S^{zz}(\boldsymbol{q}, \omega)$ exhibits a central peak as first predicted by Villain [1]. In this paper, we shall be concerned with the spin-wave response only in which transitions to the excited states occur from the ground state and so can be described by a $T = 0$ theory.

The compounds $CsCoCl_3$ and $CsCoBr_3$ have been studied through a variety of experimental techniques such as neutron scattering [4, 5, 10–13], ESR [14, 15], NMR [16] and Raman scattering [3, 17]. A large body of experimental data thus exists with which theoretical results can be compared. Both the compounds have a hexagonal structure

0953-8984/96/030351+10$19.50

consisting of chains of magnetic Co^{2+} ions. The exchange interactions within a chain are much stronger than those between chains, making a linear-chain description possible. The compounds show successive phase transitions at temperatures T_{N1} and T_{N2}. For temperatures $T > T_{N1}$, this system is in a paramagnetic phase. The intermediate phase between T_{N1} and T_{N2} is a partially ordered phase with two thirds of the magnetic chains ordering antiferromagnetically. For $T < T_{N2}$, a ferrimagnetic phase is obtained in which all the magnetic chains order in a collinear ferrimagnetic arrangement. Various experiments show evidence of the propagation of DWPs in the intermediate and paramagnetic phases. ESR signals in the 3D ordered phase indicate [18] the presence of domain walls although their detailed dynamics are not obtained from the ESR experiment. There is thus no doubt that the spin dynamics of the compounds described as Ising-like antiferromagnets are governed by domain walls, especially in the intermediate and paramagnetic phases. We shall confine our discussion to the paramagnetic phase in which a linear-chain description is quite good. A significant feature of the spin-wave response of $S^{xx}(\boldsymbol{q}, \omega)$ in the paramagnetic phase and near the zone centre is that the spectral weights are heavily concentrated towards the lower-energy side. This asymmetry in lineshape at low T cannot be explained by the first-order perturbation theory of IS. Nagler *et al* [4] added a staggered field term

$$H_S = h \sum_i (-1)^i S_i^z \tag{2}$$

to the Hamiltonian in (1). The staggered field h has two contributions h_0 and h_{ic}. The first contribution originates from taking account of the exchange mixing of higher levels within the ground doublet. The second contribution arises out of the effect of interchain exchange interactions which are important even above but close to T_{N1}. The interchain interactions treated in the mean-field approximation give rise to the staggered field term h_{ic}. The effective $S = \frac{1}{2}$ Hamiltonian containing both H (equation (1)) and H_S (equation (2)) is still defined in one dimension. Using this Hamiltonian, Nagler *et al* could explain the asymmetry in the lineshape of $S^{xx}(\boldsymbol{q}, \omega)$ near the zone centre. Their theory, however, predicted several split peaks of $S^{xx}(\boldsymbol{q}, \omega)$ the existence of which has not been experimentally verified. Matsubara and Inawashiro (MI) [8, 9] have included a weak next-nearest-neighbour (NNN) ferromagnetic (FM) interaction H_F in the Hamiltonian H in (1):

$$H_F = -2J' \sum_i [S_i^z S_{i+2}^z + \varepsilon (S_i^x S_{i+2}^x + S_i^y S_{i+2}^y)] \qquad |J'| \ll J \qquad \varepsilon \ll 1. \tag{3}$$

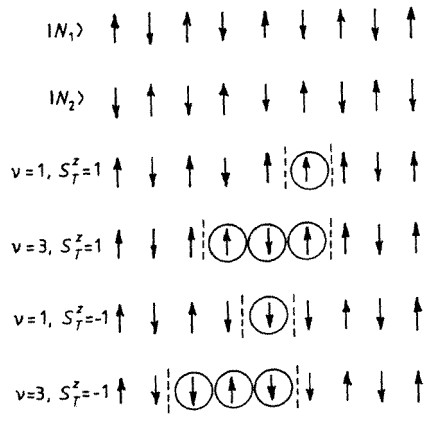

Figure 1. Néel states and DWP states for $S_T^z = \pm 1$. The broken lines indicate the position of domain walls.

They have shown the existence of bound states of DWPs besides the free DWP states. They have further shown that at $T = 0$, when J' is FM ($J' > 0$), the transverse correlation function $S^{xx}(\boldsymbol{q}, \omega)$ exhibits a sharp peak at lower energy while the peak occurs at a higher energy for $J' < 0$. The results for $J' > 0$ are in good agreement with experimental data.

In this paper, we consider the fully anisotropic Ising-like AFM $S = \frac{1}{2}$ Hamiltonian in one dimension and show that using this Hamiltonian some of the results obtained by MI such as the asymmetry of the lineshape of $S^{xx}(\boldsymbol{q}, \omega)$ and bound states of DWPs can be derived. In section 2, the theory and the results for the eigenvalues of the DWP continuum and DWP bound states are derived. In section 3, the transverse correlation function $S^{xx}(\boldsymbol{q}, \omega)$ is calculated and also the dominant spin-wave dispersion obtained from the peak positions of the correlation functions. Section 4 contains a discussion of the results obtained.

2. Domain-wall pair states

The fully anisotropic Ising-like Heisenberg Hamiltonian in one dimension is given by

$$\begin{aligned} H_{xyz} &= 2\sum_{i=1}^{N}(J_x S_i^x S_{i+1}^x + J_y S_i^y S_{i+1}^y + J_z S_i^z S_{i+1}^z) \\ &= 2J\sum_{i=1}^{N}\left[S_i^z S_{i+1}^z + \frac{\varepsilon_1}{2}(S_i^- S_{i+1}^+ + S_i^+ S_{i+1}^-) + \frac{\varepsilon_2}{2}(S_i^+ S_{i+1}^+ + S_i^- S_{i+1}^-)\right] \end{aligned} \tag{4}$$

$$J = J_z \qquad \varepsilon_1 = (J_x + J_y)/2J \qquad \varepsilon_2 = (J_x - J_y)/2J \qquad \varepsilon_1, \varepsilon_2 \ll 1.$$

Hamiltonian (1) is a special case of (4) when $J_x = J_y$. Since the anisotropy constants ε_1 and ε_2 are much less than 1, the Ising part H_{zz} of H_{xyz} can be treated as the unperturbed Hamiltonian and the rest of the Hamiltonian, H_{xy}, treated as perturbation, i.e.

$$H_{xyz} = H_{zz} + H_{xy}. \tag{5}$$

For this Hamiltonian a periodic boundary condition is assumed, i.e. $N + 1 \equiv 1$, where N is the total number of spins. The ground state of H_{zz} is doubly degenerate and so are the Néel states $|N_1\rangle$ and $|N_2\rangle$ shown in figure 1. From these two states, one can construct two translationally symmetric ground states

$$\phi^+ = \frac{1}{\sqrt{2}}(|N_1\rangle + |N_2\rangle) \qquad \phi^- = \frac{1}{\sqrt{2}}(|N_1\rangle - |N_2\rangle) \tag{6}$$

with momentum wavevectors $q = 0$ and π respectively. Lowest-lying excited states can be obtained from the Néel state by flipping a block of ν adjacent spins (figure 1), giving rise to DWP states. The broken lines indicate the positions of the domain walls. We choose a set of basis states for odd ν describing propagating DWPs with wavevector q:

$$|\nu, q\rangle_\pm = \frac{1}{\sqrt{2N}}\sum_j \exp(\mathrm{i}qr_j)\left(S_j^+\prod_{l=1}^{(\nu-1)/2} S_{j+2l-1}^- S_{j+2l}^+ + S_j^-\prod_{l=1}^{(\nu-1)/2} S_{j+2l-1}^+ S_{j+2l}^-\right)\phi^\pm. \tag{7}$$

A set of basis states can similarly be defined for even ν, which gives rise to the same excitation spectrum as in the case of odd ν. Within the space of basis states defined by (7), the ground-state energy in second-order perturbation theory is

$$E_g = -\frac{NJ}{2}(1 + \varepsilon_1^2). \tag{8}$$

The ground-state degeneracy is not lifted in this order. The matrix elements of H_{xyz} in the set of basis states are given by

$${}_+\langle\nu, q|H_{xyz}|\nu, q\rangle_+ = \begin{cases} 2J(1 + \varepsilon_1^2) + 2J\varepsilon_2\cos q = A_0 & \text{for } \nu = 1, N-1 \\ 2J(1 + \frac{3}{2}\varepsilon_1^2) = A & \text{otherwise.} \end{cases} \tag{9}$$

The diagonal elements have been calculated with respect to the ground-state energy E_g in (8). The off-diagonal elements are given by

$$ {}_+\langle \nu, q|H_{xyz}|\nu', q\rangle_+ = \begin{cases} V \\ V^* \end{cases} \quad \text{for} \begin{cases} \nu' = \nu - 2 \\ \nu' = \nu + 2 \end{cases} \tag{10} $$

$$ V = 2J\varepsilon_1[1 + \exp(2\mathrm{i}qa)]. $$

a is the lattice constant which is taken hereafter as 1. Identical results are obtained for the states $|\nu, q\rangle_-$. The off-diagonal terms have been calculated up to first order in the anisotropy constants following MI [8, 9] so that a comparison with their results is possible. The first excited eigenstates can be constructed as an appropriate linear combination of the DWP states:

$$ |\Psi(q)\rangle_\pm = \sum_{\nu=1}^{N/2} b_{2\nu-1} \exp[\mathrm{i}(2\nu - 1)\alpha]|2\nu - 1\rangle_\pm. \tag{11} $$

With the choice $\exp(2\mathrm{i}\alpha) = (V/V^*)^{1/2}$, the following equations for the coefficients b_ν are obtained:

$$ \begin{aligned} &\lambda b_1 = A_0 b_1 + \bar{V} b_3 && \text{for } \nu = 1 \\ &\lambda b_\nu = A b_\nu + \bar{V}(b_{\nu-2} + b_{\nu+2}) && \text{for } \nu \neq 1, N-1 \\ &\lambda b_{N-1} = A_0 b_{N-1} + \bar{V} b_{N-3} && \text{for } \nu = N-1 \end{aligned} \tag{12} $$

where λ is the eigenvalue and $\bar{V} = 2\varepsilon_1 J|\cos q|$. MI [8, 9] have derived an identical set of equations with A_0 and A given by

$$ \begin{aligned} A_0 &= 2J(1 + \varepsilon^2) + 2J'(1 - \varepsilon\cos(2q)) \\ A &= 2J(1 + \tfrac{3}{2}\varepsilon^2) + 4J' \end{aligned} \tag{13} $$

where J' is the NNN FM interaction (equation (3)). Following the MI derivation, the solutions are of two categories

(i) *Free DWP states.* These states give rise to the continuum of excited states with a lower and upper boundary and eigenvalue

$$ \lambda = A + 2\bar{V}\cos(2p) \tag{14} $$

with

$$ b_\nu = \frac{1}{\sqrt{N}}\{\exp[\mathrm{i}p(\nu + 1)] - \exp(\mathrm{i}\varphi_\mu)\exp[-\mathrm{i}p(\nu + 1)]\} \tag{15} $$

Here $p = (\pi\mu + \varphi_\mu)/(N + 1)$, $\mu = 1, 2, 3, \ldots, N/2$ and φ_μ is approximately given by

$$ \varphi_\mu = 2\tan^{-1}\left[\frac{\bar{A}\sin(2\pi\mu/(N+2))}{\bar{V} + \bar{A}\cos(2\pi\mu/(N+2))}\right] \tag{16} $$

where $\bar{A} = A - A_0 = -2J\varepsilon_2\cos q$.

When $\bar{V} > |\bar{A}|$, all the solutions belong to this category. When $\bar{V} < |\bar{A}|$, $N/2 - 2$ solutions are of this category and the remaining two solutions belong to the other category. The continuum eigenvalue λ given in (14) is the same as obtained by IS [2], since the energy does not have a first-order contribution in ε_2. However, the b_ν-values are different since $\exp(\mathrm{i}\varphi_\mu)$ deviates significantly from 1. It is the change in $|b_\mu|$ which is responsible for the asymmetry in $S^{xx}(\boldsymbol{q}, \omega)$.

(ii) *DWP bound states.* In this case, $|b_\mu|$ decreases as ν increases from 1 to $N/2$. Again, following MI, the eigenvalue

$$ \lambda = A_0 - \frac{\bar{V}^2}{\bar{A}} \tag{17} $$

and

$$b_\nu = \left[\frac{\bar{A}^2 - \bar{V}^2}{\bar{A}^2}\right]^{1/2}\left[-\frac{\bar{V}}{\bar{A}}\right]^{(\nu-1)/2}. \tag{18}$$

Another solution with the same eigenvalue is obtained by replacing b_ν by $b_{N-\nu}$.

We now take into account the fact that there are two ground states ϕ^+ and ϕ^- with momenta 0 and π, respectively. Both the ground states lead to the same solutions. However, the momentum wavevector q of the DWPs should be measured with respect to that of the ground state. For ϕ^+, equations (14) and (17) for λ remain unchanged. When the ground state is ϕ^-, q is to be redefined as $q - \pi$. Equations (14) and (17) are still valid but q is replaced by $q - \pi$ in A_0 and $\bar{A}$.

Figure 2 shows a plot of the spin-wave excitation continuum (broken curves) and the bound-state energy (solid curves) for $\varepsilon_1 = 0.05$ and $\varepsilon_2 = 0.1$. In the DWP bound states, the walls do not separate beyond a distance

$$d = \frac{1}{p} = \frac{2}{\ln[|\bar{A}|/\bar{V}]}. \tag{19}$$

One finds the existence of two bound-state branches a and b the energies of which lie both below and above the continuum. For the a branch, the energy lies below the continuum for $q < \pi/2$ and above the continuum for $q > \pi/2$. The reverse is true for the b branch. In the case of the MI Hamiltonian, there is just one bound-state branch lying below the continuum $J' > 0$ and above for $J' < 0$.

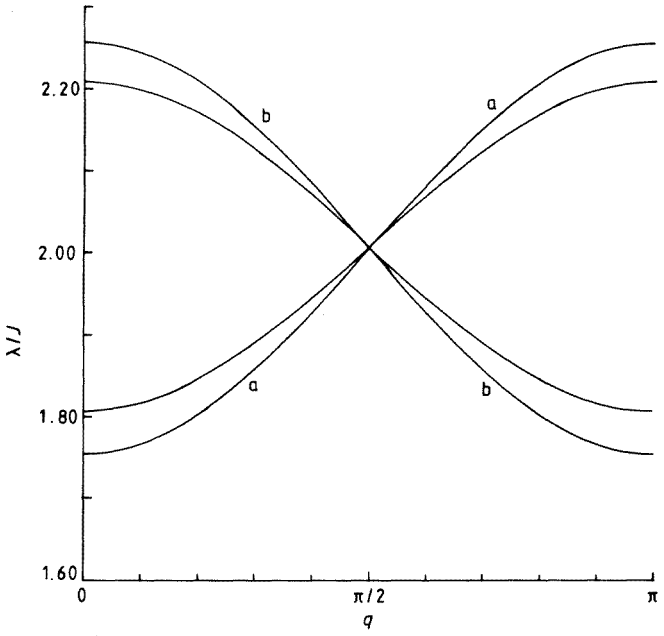

Figure 2. Spin-wave excitation continuum and DWP bound-state energy in units of J for $\varepsilon_1 = 0.05$ and $\varepsilon_2 = 0.1$.

3. Transverse correlation function $S^{xx}(q,\omega)$ at $T = 0$ K

The transverse correlation function $S^{xx}(\boldsymbol{q},\omega)$ at $T = 0$ K can be written as

$$S^{xx}(\boldsymbol{q},\omega) = \frac{1}{d}\sum_{\lambda}\sum_{i}^{d}|\langle\Psi_\lambda|S^x(q)|G_i\rangle|^2\delta(\omega - E_q + E_g) \tag{20}$$

where the ground state $|G_i\rangle$ is d-fold degenerate with eigenvalue E_g and the Ψ_λ are the excited eigenstates with eigenvalues E_λ. In this case the ground state is doubly degenerate even in second-order perturbation theory and $d = 2$. Equation (20) can further be written as

$$\begin{aligned} S^{xx}(\boldsymbol{q},\omega) &= \tfrac{1}{2}\sum_{\lambda}\{|\langle\Psi_\lambda|S^x(q)|G^+\rangle|^2 + |\langle\Psi_\lambda|S^x(q)|G^-\rangle|^2\}\delta(\omega - E_\lambda + E_g) \\ &= \tfrac{1}{2}[S^{xx}_+(\boldsymbol{q},\omega) + S^{xx}_-(\boldsymbol{q},\omega)] \end{aligned} \tag{21}$$

where $|G^+\rangle$ and $|G^-\rangle$ are the two ground states. Also

$$S^x(q) = \frac{1}{2\sqrt{N}}\sum_{\lambda}\exp(\mathrm{i}qr_j)(S_j^+ + S_j^-). \tag{22}$$

Consider the unperturbed ground state ϕ^+. The ground state $|G^+\rangle$ to first order in ε_1 and ε_2 is given by

$$|G^+\rangle = \phi^+ + \sum_{\lambda}{}' \frac{\langle K|H_{xy}|\phi^+\rangle|K\rangle}{E_0 - E_k} \tag{23}$$

where E_0 is the unperturbed ground-state energy equal to $-JN/2$. E_k is the energy of the unperturbed eigenstate $|K\rangle$ and the prime indicates $|K\rangle \neq \phi^+$:

$$|G^+\rangle = \phi^+ + J\varepsilon_1\sum_i(S_i^+S_{i+1}^- + S_i^-S_{i+1}^+)|\phi^+\rangle \Big/ -2J.$$

There is no first-order contribution in ε_2 as $S_i^+S_{i+1}^+ + S_i^-S_{i+1}^i$ acting on ϕ^+ gives zero:

$$S^x(q)|G^+\rangle = \tfrac{1}{2}\left[(1 - \varepsilon_1\cos q)|1q\rangle_+ - \frac{V}{2J}|3q\rangle_+\right]. \tag{24}$$

$|\nu,q\rangle_+$ is given by (7). Using (21) and (24) and the expression for Ψ_λ from (11), we get

$$\begin{aligned} S^{xx}_+(\boldsymbol{q},\omega) = -\frac{1}{4\pi}\,\mathrm{Im}\Bigg\{&(1 - \varepsilon_1\cos q)^2G_{11} + \frac{|V|^2}{4J^2}G_{33} - \frac{[1 - \varepsilon_1\cos q]V}{2J}G_{13} \\ &- \frac{[1 - \varepsilon_1\cos q]V^*}{2J}G_{31}\Bigg\}. \end{aligned} \tag{25}$$

Im denotes the imaginary part,

$$G_{(i,j)} = \left\langle i\left|\frac{1}{\omega - H_{xyz}(q) + \mathrm{i}\delta}\right|j\right\rangle \qquad (\delta \to 0^+) \tag{26}$$

is the Green function defined with (9) and (10). $G_{(i,j)}$ can be evaluated by techniques similar to those used for the evaluation of Green functions in the NN tight-binding model with free ends [2]. We list the Green functions as follows:

$$\begin{aligned} G_{11} &= \frac{2\Omega_0 - \Omega - \mathrm{i}\sqrt{4|V|^2 - \Omega^2}}{2[|V|^2 - \Omega_0\Omega + \Omega_0^2]} \\ G_{13} &= \frac{G_0}{V} \qquad G_{31} = \frac{G_0}{V^*} \qquad G_{33} = \frac{G_0\Omega_0}{|V|^2} \end{aligned} \tag{27}$$

where

$$G_0 = \frac{\Omega_0\Omega - 2|V|^2 - \mathrm{i}\Omega_0\sqrt{4|V|^2 - \Omega^2}}{2[|V|^2 - \Omega_0\Omega + \Omega_0^2]}$$
$$\Omega_0 = \omega - A_0 \qquad \Omega = \omega - A.$$

$S_{-}^{xx}(\boldsymbol{q}, \omega)$ has an expression similar to (25) but with q replaced by $q - \pi$. Using the expressions for the Green functions in (27), one finally obtains

$$S^{xx}(\boldsymbol{q}, \omega) = \frac{1}{2}\left\{ \frac{\sqrt{4|V|^2 - \Omega^2}}{8\pi(|V|^2 - \Omega_0\Omega + \Omega_0^2)} \left[(1 - \varepsilon_1 \cos q)^2 - \frac{\Omega_0}{J}(1 - \varepsilon_1 \cos q) + \frac{\Omega_0^2}{4J^2} \right] \right.$$
$$\left. + \frac{\sqrt{4|V|^2 - \Omega'^2}}{8\pi(|V|^2 - \Omega_0'\Omega' + \Omega_0'^2)} \left[(1 + \varepsilon_1 \cos q)^2 - \frac{\Omega_0'}{J}(1 + \varepsilon_1 \cos q) + \frac{\Omega_0'^2}{4J^2} \right] \right\} \tag{28}$$

where

$$\Omega_0' = \Omega_0(q \to q - \pi) \qquad \Omega' = \Omega(q \to q - \pi). \tag{29}$$

The wavevector q is measured with respect to that of the ground state. In deriving the expression for $S^{xx}(\boldsymbol{q}, \omega)$, only the contribution for the continuum of excited states has been calculated. The bound states also contribute to the correlation function and appear as sharp peaks at the bound-state energies. In figures 3 and 4, $S^{xx}(\boldsymbol{q}, \omega)$ is plotted for $q = \pi$ (zone centre) and $q = 4\pi/5$ with $\varepsilon_1 = 0.095$ and $\varepsilon_2 = 0.065$. For these parameter values, $\bar{V}$ is not less than $|\bar{A}|$ and so there are no DWP bound states. The plots are clearly asymmetric towards the lower energies. In figure 5, the dispersion of the peak positions of $S^{xx}(\boldsymbol{q}, \omega)$ for various values of q are shown and compared with the experimental results (open circles) of Satija *et al* [10].

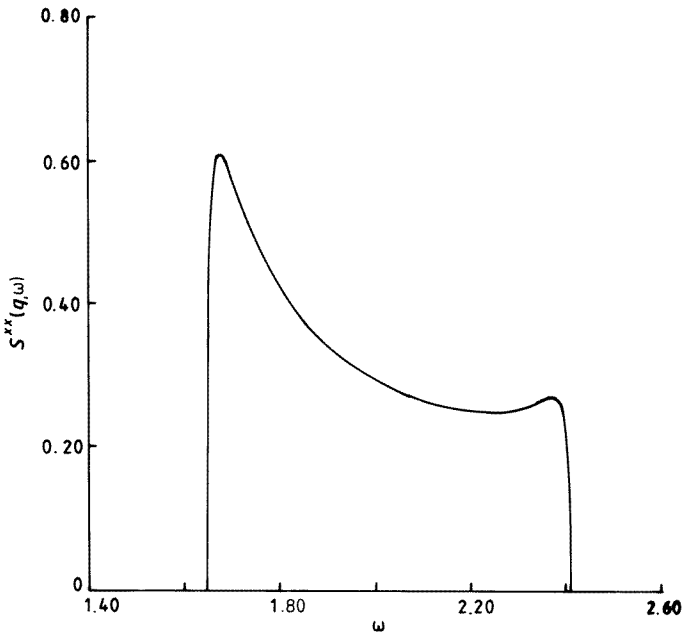

Figure 3. $S^{xx}(\boldsymbol{q}, \omega)$ at $T = 0$ for $\varepsilon_1 = 0.095$, $\varepsilon_2 = 0.065$ and $q = \pi$.

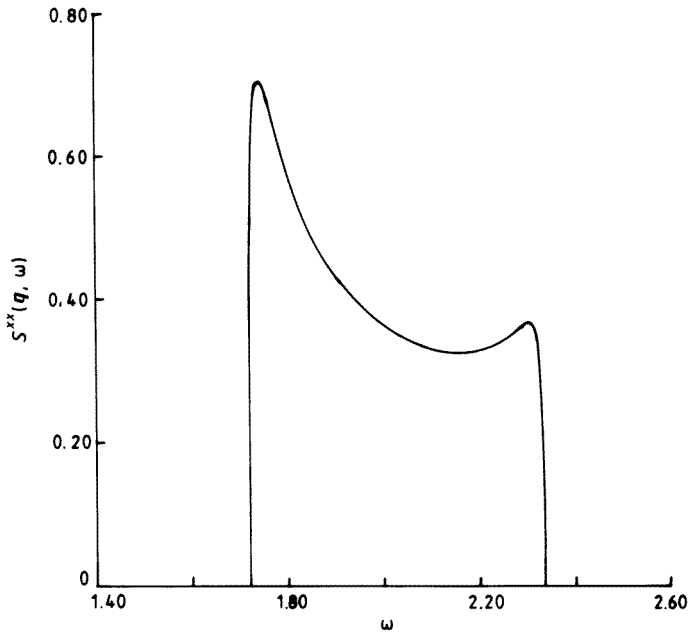

Figure 4. $S^{xx}(\boldsymbol{q}, \omega)$ at $T = 0$ for $\varepsilon_1 = 0.095$, $\varepsilon_2 = 0.065$ and $q = 4\pi/5$.

4. Discussion of results

We have shown using the fully anisotropic Ising-like Heisenberg Hamiltonian that some of the results of the MI theory, in which a NNN FM interaction is assumed besides the usual NN AFM interaction, can be qualitatively reproduced. These include the formation of the DWP bound states and an asymmetry in the lineshape of the transverse correlation function $S^{xx}(\boldsymbol{q}, \omega)$ at the zone centre. There are, however, a number of differences. The MI theory gives rise to a single bound-state branch whereas in the present case two branches are obtained. No experimental results are as yet available on the effect of bound states on the thermodynamic and dynamic properties of the experimental systems $CsCoCl_3$ and $CsCoBr_3$. So one cannot comment on which bound-state description is closer to experimental results. The bound-state formation is more restricted and has less dispersion in the case of H_{xyz} than in the case of the MI Hamiltonian. The transverse correlation function $S^{xx}(\boldsymbol{q}, \omega)$ in the present case has a two-peak structure. Near the zone centre, the intensity of the peak towards the low-energy side is greater and an asymmetry in the lineshape is clearly evident. The MI lineshape has a single peak with asymmetry towards the lower energy. The double-peaked structure in the correlation functions of AFM chains has been reported earlier [19]. The experimental data presented in [11, 20] indicate the existence of weak resonances at higher frequencies. There is, however, no definite experimental results on the existence of a second peak of magnetic origin in the transverse correlation function of $CsCoCl_3$ and $CsCoBr_3$. The dispersion relation of the peak frequencies of $S^{xx}(\boldsymbol{q}, \omega)$ (figure 5) of H_{xyz} does not show very good agreement with the experimental data. This may be due to the limitations of a first-order perturbation theory in the calculation of $S^{xx}(\boldsymbol{q}, \omega)$. Bose and Chatterjee [6] using second-order perturbation theory in the calculation of $S^{xx}(\boldsymbol{q}, \omega)$ showed that a marked improvement in the fitting of the peak frequencies to experimental data occurs. Inclusion

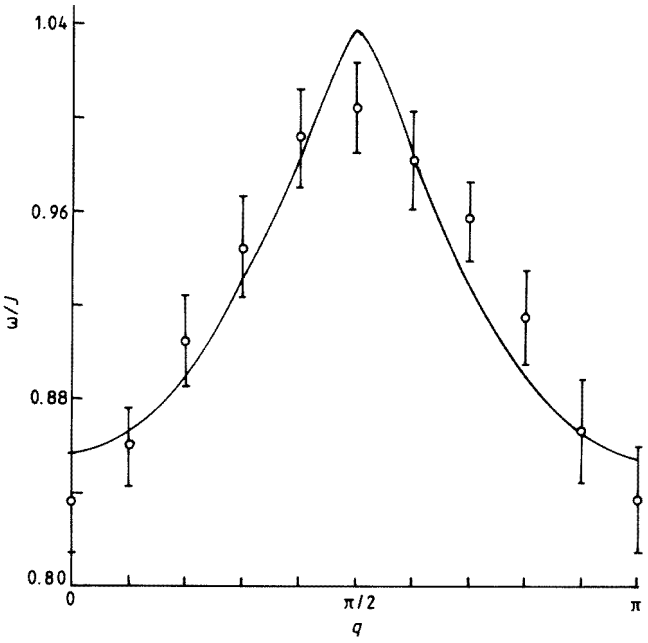

Figure 5. Dispersion of peak frequencies of $S^{xx}(\boldsymbol{q}, \omega)$: ○, experimental data of Satija *et al* [10].

of further terms in the Hamiltonian such as the staggered field term of Nagler *et al* [4] may also improve the fitting to experimental results. The present perturbative scheme is not of general applicability because of the use of a restricted set of basis states as in (7). Adoption of cluster algorithms [21] may lead to a more general approach.

The restriction to the subspace of states of type (7) has the effect that the continuum energy eigenvalue λ given by (14) is independent of ε_2 to the first order in ε_2. The expression for λ is thus identical with that obtained in the case $\varepsilon_2 = 0$ when the energy is calculated to first order in ε_1. For this case, the exact Bethe *ansatz* result [22] is known which, for $\varepsilon_1 \to 0$ and to first order in ε_1, is identical with (14) [23, 24]. Exact results corresponding to the DWP bound-state energy given in (17) are not known.

Apart from relevance to experimental systems such as $CsCoCl_3$ and $CsCoBr_3$, the present study is intended to provide insights about the spin dynamics of fully anisotropic Ising-like AFM systems. The ground-state energy and low-lying excitation spectrum of the fully anisotropic Heisenberg Hamiltonian are known exactly because of the mapping between the fully anisotropic Hamiltonian and the exactly solvable eight-vertex model [22, 25]. The dynamical correlation functions are, however, not known exactly because of a lack of knowledge of the exact wavefunctions. In [19] the correlation functions for the various special cases of the general anisotropic Hamiltonian are discussed. The Ising-like limit in which we are interested is, however, only briefly discussed. Our calculations provide us with some physical insights about spin dynamics in Ising-like fully anisotropic AFM systems which are not obvious from the mapping onto the eight-vertex model. An important feature is the double degeneracy of the ground state with two different momentum wavevectors. This is responsible for the two branches of bound states and also two peaks in the transverse correlation functions.

The non-triviality of the double degeneracy of the ground state can be rigorously

demonstrated in the special case of H_{xyz} in (4) with $\varepsilon_1 = 0$. Bose *et al* [26] have shown that the Néel states $|N_1\rangle$ and $|N_2\rangle$ are the exact ground states in this case. The Hamiltonian is unitarily related to the FM Heisenberg Hamiltonian and so has the same spectrum. When the ground state is $\phi^{\pm}$, the exact excitation spectrum is given by

$$e^{\pm} = 1 \mp \varepsilon_2 \cos q \tag{30}$$

where q is measured with respect to the ground-state wavevector. Thus there are two branches in the excitation spectrum. The lowest excitation spectrum is given by

$$e = \begin{cases} 1 - \varepsilon_2 \cos q \\ 1 + \varepsilon_2 \cos q \end{cases} \qquad \text{for} \begin{cases} 0 \leqslant q \leqslant \dfrac{\pi}{2} \\ \dfrac{\pi}{2} \leqslant q \leqslant \pi. \end{cases} \tag{31}$$

The exact excited states with eigenvalues $e^{\pm}$ are simply propagating DWP states with unit length ($\nu = 1$ in (7)). In this case there is no continuum of excited states. The continuum is obtained only when $\varepsilon_1 \neq 0$. On the other hand, when $\varepsilon_2 < \varepsilon_1$ or $\varepsilon_2 = 0$ and J' in the MI Hamiltonian is zero, bound states of DWPs do not occur. The evidence of DWP bound states from experimentally measurable quantities is, however, yet to be obtained for a real system.

References

[1] Villain J 1975 *Physica* B **79** 1
[2] Ishimura N and Shiba H 1980 *Prog. Theor. Phys.* **63** 745
[3] Shiba H 1980 *Prog. Theor. Phys.* **64** 466
[4] Nagler S E, Buyers W J L, Armstrong R L and Briat B 1983 *Phys. Rev.* B **27** 1784
[5] Nagler S E, Buyers W J L, Armstrong R L and Briat B 1983 *Phys. Rev.* B **28** 3873
[6] Bose I and Chatterjee S 1983 *J. Phys. C: Solid State Phys.* **16** 947
[7] Bose I and Chatterjee S 1983 *J. Phys. C: Solid State Phys.* **16** 6681
[8] Matsubara F and Inawashiro S 1989 *J. Phys. Soc. Japan* **58** 4284
[9] Matsubara F and Inawashiro S 1991 *Phys. Rev.* B **43** 796
[10] Satija A K, Shirane G, Yoshizawa H and Hirakawa K 1980 *Phys. Rev. Lett.* **44** 1548
[11] Yoshizawa H, Hirakawa K, Satija A K and Shirane G 1981 *Phys. Rev.* B **23** 2298
[12] Baucher J P, Regnault L P, Rossat-Mignod J, Henry Y, Bouillot J and Stirling W G 1985 *Phys. Rev.* B **31** 3015
[13] Buyers W J, Hogan M J, Armstrong R L and Briat B 1986 *Phys. Rev.* B **33** 1727
[14] Adachi K 1981 *J. Phys. Soc. Japan* **50** 3904
[15] Boucher J P, Rius G and Henry Y 1987 *Europhys. Lett.* **4** 1073
[16] Adachi K, Hamashima M, Ajiro Y and Mekata M 1979 *J. Phys. Soc. Japan* **47** 780
[17] Lehmann W P, Breitling W and Weber R 1981 *J. Phys. C: Solid State Phys.* **14** 4655
[18] Kohmoto T, Goto T, Maekawa S, Fujiwara L, Fukuda Y, Kumitomo N and Mekata M 1994 *Phys. Rev.* B **49** 6028
[19] Mohan M and Müller G 1983 *Phys. Rev.* B **27** 1776
[20] Nagler S E, Buyers W J L and Armstrong R L 1981 *J. Appl. Phys.* **52** 1971
[21] Kawashima N and Gubernatis J B 1995 *Phys. Rev.* E **51** 1547
[22] Johnson J D, Krinsky S and McCoy B M 1973 *Phys. Rev.* A **8** 2526
[23] Fowler M and Puga M W 1978 *Phys. Rev.* B **18** 421
[24] Mikeska H J and Steiner M 1991 *Adv. Phys.* **40** 191
[25] Baxter R J 1972 *Ann. Phys., NY* **70** 323
[26] Bose I, Chatterjee S and Majumdar C K 1984 *Phys. Rev.* B **29** 2741